Analysis of Inclusive Distributions Using a Statistical Approach*

Dennis Sivers and Gerald H. Thomas
High Energy Physics Division, Argonne National Laboratory, Argonne, Illinois 60439
(Received 15 May 1972)

A statistical approach to production amplitudes is used to investigate the consequences for inclusive spectra due to (1) conservation laws, (2) small transverse momenta, (3) small average inelasticity, and (4) an asymptotically constant inelastic cross section. An analytic approximation of phase-space integrals is employed. Features of one- and two-particle inclusive spectra are discussed in terms of their exclusive components; both analytic and numerical results are presented. As a specific example of the approach, the rapidity distributions for $pp \to \pi^-\pi^- X$ are compared with data at 21 GeV/c. The above assumptions cannot account for some features of the $\pi^-\pi^-$ spectra, indicating the necessity for additional dynamic input.

I. INTRODUCTION

Recent papers on two-particle inclusive distributions and correlation functions[1-4] raise an important question of whether such quantities show dynamic features not already known from one-particle spectra and exclusive data. We shall attempt to analyze this question by means of a calculation involving a simple generalization of Fermi's statistical model.[5] Our approach differs from a Feynman gas-liquid analogy[6-8] or a Mueller-type analysis of discontinuities[9-10] in that we propose to discuss the inclusive distributions in terms of a model constructed for each of the exclusive components. As argued by Berger and Krzywicki,[11] this component approach can give useful insight into inclusive distributions, insight otherwise difficult to obtain. Constructing a statistical model which embodies the known features of the data is one way of separating the known from the unknown in a relatively unbiased way. A comparison of such a model with data will thus reveal the sufficiency or insufficiency of the initial assumptions. This method of separating new dynamic effects from kinematic[5,12] or phase-space reflections of the original dynamic assumptions[13-17] has a long tradition in high-energy physics.

The first step in constructing a statistical model is to decide what general features it should have. We shall require of our model the following.

(1) Agreement with the conservation of isospin, including charge conservation, and with energy-momentum conservation.

(2) A transverse-momentum spectrum which is quickly damped, producing a small average transverse momentum.

(3) A small average inelasticity η, where η is the fraction of the total energy carried off by the secondary, or nonleading, particles.

(4) A total inelastic cross section which is approximately independent of energy.

These four properties are generally recognized to be reasonable empirically. In addition, they are common to a number of the currently popular models such as the multiperipheral model,[18-19] bremsstrahlung model,[15,20] and the diffractive fragmentation[21] or nova models.[22] We note that, in general, these models are in no way equivalent. Nevertheless, our approach enables us to verify that the success of these models in describing data in certain regions of phase space is a direct consequence of the above set of common assumptions.

For convenience, we call the statistical model having the above features an independent-emission model (IEM). Given the IEM for each exclusive matrix element, all of the calculations necessary to obtain one- and two-particle inclusive distributions can be done using standard Monte Carlo techniques for phase-space integrals.[23] However, it is a secondary purpose of this paper to show that in practice one need not use such techniques. Although the thought needed to employ Monte Carlo methods is usually minimal, the computations themselves can be very costly. Moreover, standard Monte Carlo programs are complex, making it often difficult to obtain physical insight into the results. An alternative is an elegant method proposed by Lurçat and Mazur[24] (LM) which gives an analytic approximation of phase-space integrals, good at all energies. This approximation produces an asymptotic expansion for the integrals valid when the number of produced particles is large, but when the errors are handled correctly the estimate may be adequate at small multiplicities. Moreover, the mathematics of the method bears a close correspondence to ordinary statistical mechanics. This correspondence may be useful in obtaining physical insight into the results.

In its original form, the method applied to phase-

space integrals where the S matrix factorized and was Lorentz-invariant. For our purposes, although the momentum dependence of the S matrix factorizes, there is only invariance with respect to boosts along, and rotations about, a fixed direction. For such integrals we follow Krzywicki's generalization of the method.[14,25] The errors made in the approximation of the integrals depend on the form of the matrix element. As an illustration of the type of errors which occur, we compare the estimate for elastic scattering with the exact form (see Appendix).

The main result of our calculation is a comparison of the $pp \to \pi^-\pi^- X$ inclusive distribution as a function of rapidities at 21 GeV/c. The predictions of the IEM for the $\pi^-\pi^-$ distributions are particularly interesting since this system is thought to contain no resonances or strong final-state interactions, so that we are looking directly at correlations due to the production process.

In Sec. II, the IEM and formulas for its evaluation are summarized. In Sec. III, analytic results are obtained in the high-energy limit. In Sec. IV, numerical results are given and compared with data. A discussion of other models, or previously published results, is included where relevant.

II. THE MODEL AND EVALUATION OF PHASE-SPACE INTEGRALS

To carry out our investigation into the dynamics of inclusive distributions, we construct an independent-emission model (IEM) for the reactions

$$p+p \to N+N+n\pi\,. \tag{2.1}$$

Since, experimentally, the number of produced kaons is small compared to the number of pions,[26] we feel justified in leaving out other final states.

A. Definition of the Model

The model is defined in terms of the modulus squared of the S matrix for reaction (2.1):

$$|S_{n+2}|^2 = s^{\delta}\frac{z^n}{n!}W(n_+,n_-,n_0)\prod_{i=1}^{n+2} f_i(p_i)\,. \tag{2.2}$$

The significance and definition of quantities in this equation are as follows:

(1) Assuming a factorizable form for the momentum dependence of the S matrix, and taking the probability for producing n pions proportional to z^n, we incorporate the basic statistical assumptions due to Fermi. Here, z is a parameter to be determined by experiment.

(2) The assumption that the pion transverse-momentum distributions are sharply cut off is implemented by taking for each pion in (2.2)

$$f_\pi(q) = \exp(-R^2 q_T^{\,2})\,. \tag{2.3}$$

This is the only dependence on the pion momenta which the model contains. This particular form of transverse-momentum damping was chosen partly for convenience and partly because it emerges from analyses of the dual-resonance model.[10] *A priori*, other forms would do equally well.

(3) The assumption of small inelasticity for the through-going nucleons means that, on the average, the pions have only a small fraction, η, of the available c.m. energy. This constraint is also called the leading-particle effect. For our purposes, it is conveniently parametrized by taking for the nucleons in (2.2) an f_i of the form

$$f_N(p) = \exp(2\lambda\cdot p s^{-1/2} - R^2 p_T^{\,2})\,, \tag{2.4}$$

where λ^μ is a four-vector which, in the c.m. frame, has only a time component (λ^0). For simplicity, the transverse-momentum cutoff of the nucleons is chosen to be of the same form as that for the pions, although there is no particularly compelling reason to think it so. Weighting the energies of the final-state nucleons in this way incorporates a t damping (where t is the square of the momentum transfer between an initial and final nucleon) different from that found from a single Regge-pole exchange. It can be argued that this is the most statistically unbiased way of enforcing the experimentally observed constraint that the fraction of energy transferred to the pions is only a slowly varying function of the energy available.[27] The appropriateness of this parametrization will be discussed in more detail when we present our numerical results.

(4) The energy dependence of $|S_{n+2}|^2$ parametrized in (2.2) by the factor s^δ is chosen to be such as to give a total inelastic cross section which is, within factors involving logarithms, asymptotically energy independent. For inclusive cross sections, s^δ is replaced by $(M^2)^\delta$ where M^2 is the missing mass. Without this factor, we would be incorporating a spurious dependence on the missing-mass variable of inclusive distributions.

(5) Energy and momentum conservation are automatically enforced by the phase-space integral

$$\Omega_n(P) = s^\delta \int \prod_{i=1}^{2}\frac{d^3p_i}{2E_i}\exp(2\lambda\cdot p_i s^{-1/2} - R^2 p_{iT}^{\,2}) \times \prod_{j=1}^{n}\frac{d^3q_j}{2\omega_j}\exp(-R^2 q_{jT}^{\,2})\,\delta^4\Big(P-\sum_{i=1}^{2}p_i-\sum_{j=1}^{n}q_j\Big)\,, \tag{2.5}$$

where $s = P^2$.

(6) Finally, isospin conservation is assumed to be valid in an average sense as in Fermi's statistical model. In terms of reaction (2.1), the assump-

tion is that all ways of forming $I=1$ from the final-state particles are equally probable. For $n_+\pi^+$, $n_-\pi^-$, and $n_0\pi^0$ in the final state ($n=n_++n_-+n_0$), this determines an isospin weight $W(n_+, n_-, n_0)$. The isospin weight can be given in closed form by a formula due to Cerulus,[28,29]

$$W(n_+, n_-, n_0) = \frac{n!}{n_+!\, n_-!\, n_0!} \times \frac{2!}{n_p! n_n!} \times 3 \times 2^{-(n_+ + n_- + 3)} \int_{-1}^{+1} dx (1+x)^{n_+ + n_- + 2} x^{n_0}\,, \tag{2.6}$$

where $n_p = 2 - n_+ + n_-$ and $n_n = n_+ - n_-$. For some final states these weights are tabulated by Bartke.[16]

Once the phase-space integrals Ω_n are specified, we calculate the total inelastic rate,

$$\Omega(s) = \sum_{n=0}^{\infty} \frac{z^n}{n!} \Big[\sum_{n_+ + n_- + n_0 = n} W(n_+, n_-, n_0) \Big] \Omega_n(s)\,, \tag{2.7}$$

which gives the total inelastic cross section by dividing by the flux. Similar formulas relate the inclusive differential rates

$$d^k\Omega \Big/ \frac{d^3q_1}{\omega_1} \cdots \frac{d^3q_k}{\omega_k}$$

to the exclusive differential rates

$$d^k\Omega_n \Big/ \frac{d^3q_1}{\omega_1} \cdots \frac{d^3q_k}{\omega_k} \qquad (n \geq k)\,.$$

From these quantities, the inclusive densities

$$\rho_k(q_1, \ldots, q_k) = \Omega^{-1}\, d^k\Omega \Big/ \frac{d^3q_1}{\omega_1} \cdots \frac{d^3q_k}{\omega_k} \tag{2.8}$$

can be calculated.

B. The Approximation of the Phase-Space Integrals

We evaluate the phase-space integrals Ω_n by a simple generalization[25] of the method proposed by Lurçat and Mazur.[24] The nucleus of the approximation is the Laplace transform of Ω_n,

$$\Phi_n(\alpha^\nu) = \int d^4P\, e^{-\alpha^\nu P_\nu} \Omega_n(P) s^{-\delta} \tag{2.9}$$

for $\alpha_0 > 0$ and $\alpha_0^2 - \alpha_L^2 - \vec{\alpha}_T^{\,2} > 0$. Using (2.5), we can write

$$\Phi_n(\alpha^\nu) = [\psi_N(\alpha_T, \xi)]^2 [\varphi_\pi(\alpha_T, \alpha)]^n = \Phi_n(\alpha_T, \alpha)\,, \tag{2.10}$$

where

$$\xi = [(\alpha_0 - 2\lambda_0/s^{1/2})^2 - (\alpha_L - 2\lambda_L/s^{1/2})^2]^{1/2}\,, \tag{2.11}$$

$$\alpha = [\alpha_0^2 - \alpha_L^2]^{1/2}\,, \tag{2.12}$$

$$\alpha_T = [\vec{\alpha}_T^{\,2}]^{1/2}\,. \tag{2.13}$$

The Laplace transform of f_π given by (2.3) is φ_π, and ψ_N is the Laplace transform of f_N in (2.4). It is easily verified that these integrals are

$$\varphi_\pi(\alpha_T, \alpha) = \pi \int d(q_T^2) \exp\{-R^2 q_T^2\} I_0(\alpha_T q_T) K_0(\alpha \kappa_\pi)\,, \tag{2.14}$$

$$\psi_N(\alpha_T, \xi) = \pi \int d(p_T^2) \exp\{-R^2 p_T^2\} I_0(\alpha_T p_T) K_0(\xi \kappa_N)\,, \tag{2.15}$$

where $\kappa_\pi = (\mu^2 + q_T^2)^{1/2}$ and $\kappa_N = (m^2 + p_T^2)^{1/2}$ are the transverse masses of the pion and nucleon, respectively. The $I_0(x)$ and $K_0(x)$ are modified Bessel functions.[30] These integrals can be evaluated to determine $\Phi_n(\alpha_T, \alpha)$ in (2.10). The rate Ω_n is then obtained using the inverse transform

$$\frac{\Omega_n(P) e^{-\alpha \cdot P}}{\Phi_n(\alpha_\mu)} = \int \frac{d^4t}{(2\pi)^4}\, e^{-iP\cdot t}\, \frac{\Phi_n(\alpha_\mu - it_\mu)}{\Phi_n(\alpha_\mu)}\,, \tag{2.16}$$

where the equation is valid for all positive time-like α_μ.

The LM approximation of (2.16) is an estimate by the method of steepest descents. Expanding

$$\ln \frac{\Phi_n(\alpha_\mu - it_\mu)}{\Phi_n(\alpha_\mu)} = -iA_n^\mu t_\mu - \tfrac{1}{2} B_n^{\mu\nu} t_\mu t_\nu + \cdots, \tag{2.17}$$

the condition $-A_n^\mu = P^\mu$ guarantees that the integrand in (2.16) is approximately Gaussian. In analogy with the proof of the central-limit theorem in mathematical statistics,[31] this method gives an estimate for the integral valid when the number of particles is large. In a frame where $P_L = 0$ and $|\vec{P}_T|$ small, the conditions on α and α_T are

$$\alpha_T \to 0\,, \tag{2.18}$$

$$P_0 = -\frac{\partial}{\partial \alpha} \ln \Phi_n(\alpha_T, \alpha) \Big|_{\alpha_T = 0}\,. \tag{2.19}$$

By analogy with statistical mechanics, we call $\Phi_n(\alpha)$ the *partition function*, and the solution, β, to (2.19) is called the inverse *temperature*. In this frame, $B_n^{\mu\nu}$ contains only diagonal components

$$B_n^{00} = \frac{\partial^2}{\partial \beta^2} \ln \Phi_n(\alpha_T, \beta) \Big|_{\alpha_T = 0}\,, \tag{2.20}$$

$$B_n^{LL} = s^{1/2}/\beta\,, \tag{2.21}$$

$$B_n^{TT} = \left(\frac{1}{\alpha_T}\right) \frac{\partial}{\partial \alpha_T} \ln \Phi_n(\alpha_T, \beta)\Big|_{\alpha_T = 0} . \tag{2.22}$$

The evaluation of (2.16) in this approximation is now straightforward; the result is

$$\Omega_n(P) = s^{\delta} \frac{\exp(\beta P_0)\Phi_n(\beta)}{(2\pi)^2 (\det B_n)^{1/2}} \exp\left(\frac{-P_T^2}{2B_{TT}}\right) \{1 + \mathcal{R}_n(\beta, P_T)\} , \tag{2.23}$$

where $\det B_n = B_n^{00} B_n^{LL} (B_n^{TT})^2$ and $\mathcal{R}_n(\beta, P_\perp)$ contains corrections from higher-order terms in the expansion (2.17). The LM analysis guarantees that, at a given energy, this correction term is $O(n^{-1/2})$ for large n. We refer the reader to Lurçat and Mazur[24] and to Krzywicki[25] for a more thorough discussion. In this paper, we will not use the correction term $\mathcal{R}_n(\beta, P_T)$ in (2.23) even though we have reason to believe that it is large for small n. In the Appendix we argue that this is justifiable.

In evaluating the exclusive rates

$$d^k \Omega_n \Big/ \left(\frac{d^3 q_1}{\omega_1} \cdots \frac{d^3 q_k}{\omega_k}\right),$$

we are confronted with integrals in which the frame $P_L = 0$ in (2.16) is not the same as the overall c.m. frame. Since the incorporation of the leading particle effect enforces, when some particles are removed, nontrivial constraints on how the remaining energy is shared among the other particles, special care must be exercised in evaluating these integrals.

Notice that with $\lambda = 0$ in (2.5), there is a recursion relation of the form[32]

$$\Omega_n(P) = \int \frac{d^3 \vec{q}}{2\omega} e^{-R^2 q_T^2} \left(\frac{s}{M^2}\right)^{\delta} \Omega_{n-1}(P - q) , \tag{2.24}$$

where $M = [(P - q)^2]^{1/2}$ is the missing mass, making it trivial to extract exclusive rates. When $\lambda \neq 0$ we notice that the Laplace transform ψ_N depends on the length ξ as shown in (2.15). Defining u as the boost variable which transforms from the c.m. frame to the frame where the longitudinal momentum of the unobserved particles vanishes, we have

$$\xi = (\alpha - 2\lambda s^{-1/2} e^{u})^{1/2} (\alpha - 2\lambda s^{-1/2} e^{-u})^{1/2} , \tag{2.25}$$

and the temperature equation, (2.19), assumes the form

$$-2 \frac{\partial \xi}{\partial \alpha} \frac{\partial}{\partial \xi} \ln \psi_N(\xi) - n \frac{\partial}{\partial \alpha} \ln \varphi_\pi(\alpha) = M_L , \tag{2.26}$$

where M_L is the (longitudinal) missing mass,

$$M_L = [(P_0 - q_0)^2 - (P_L - q_L)^2]^{1/2} . \tag{2.27}$$

III. ANALYSIS OF THE HIGH-ENERGY LIMIT

A particular advantage of the LM approximation over a Monte Carlo calculation of the phase-space integrals is that it is possible to obtain analytically the asymptotic behavior of certain inclusive quantities. These asymptotic limits will be discussed in this section, while numerical calculations where asymptotic approximations have not been made will be presented separately in Sec. IV.

We note that the high-energy limit of the phase-space integral $\Omega_n(s)$ in (2.5) depends nonuniformly on the number $n + 2$ of final-state particles. Hence, in evaluating the total inelastic rate Ω in (2.7) and the inclusive densities ρ^k in (2.8), it is not appropriate to interchange the order of the high-energy limit with the summation over n. Instead, it is convenient to introduce directly the subsidiary function:

$$Q(\alpha) = [\psi_N(\xi)]^2 \sum_{n=0}^{\infty} \frac{z^n}{n!} \times \left[\sum_{n_+ + n_- + n_0 = n} W(n_+, n_-, n_0)\right] [\varphi_\pi(\alpha)]^n . \tag{3.1}$$

In terms of our statistical-mechanics nomenclature, we will refer to this as the *grand partition function* although it is associated with a mixed system in which the number of nucleons is fixed at two, while the number of pions is undetermined.

For simplicity, we assume that the general features of charge and isospin conservation are retained if we approximate the isospin weight functions in (3.1) by their large-n form[16]

$$W(n_+, n_-, n_0) \sim \frac{n!}{n_+! n_-! n_0!} \frac{z_+^{n_+} z_-^{n_-} z_0^{n_0}}{z^n} . \tag{3.2}$$

We compensate for the lack of strict isospin conservation by introducing different z's for the different charge states of the pions. We also assume that we can allow the sum in (3.1) to run only over $n_+ = n_-$ so that there are exactly two protons in the final state.[33,34] With these approximations

$$Q(\alpha) \cong [\psi_N(\xi)]^2 \exp[z_0 \varphi_\pi(\alpha)] I_0(2(z_+ z_-)^{1/2} \varphi_\pi(\alpha)) , \tag{3.3}$$

where, again, $I_0(x)$ is a modified Bessel function, and $\xi = \alpha - 2\lambda/\sqrt{s}$.

The inverse Laplace transformation analogous to (2.16) can now be performed with Q instead of Φ_n in the integrand. The temperature equation analogous to (2.19) is

$$-2\frac{\psi_N'}{\psi_N} - z_0\varphi_\pi' - 2(z_+z_-)^{1/2}\frac{I_1(2(z_+z_-)^{1/2}\varphi_\pi)}{I_0(2(z_+z_-)^{1/2}\varphi_\pi)}\varphi_\pi'\Big|_{\alpha=\beta=\sqrt{s}}, \tag{3.4}$$

where the primes denote differentiation with respect to α. The solution to this equation gives, for large $\sqrt{s}$, a small value of β. We, therefore, utilize an asymptotic approximation for $\varphi_\pi(\alpha, \alpha_T)$ and $\psi_N(\xi, \alpha_T)$ by taking $\alpha, \alpha_T \to 0$ in the integrands (2.14) and (2.15) and using the small-x forms of the associated Bessel functions:

$$\varphi_\pi(\alpha) \sim \frac{\pi}{R^2}[-\tfrac{1}{2}\gamma - \ln(\alpha/2R) + O(\alpha^2\ln\alpha) + O(\mu^2\ln\mu^2)], \tag{3.5}$$

and

$$\psi_N(\xi) \sim \frac{\pi}{R^2}\{[-\gamma - \tfrac{1}{2}e^{R^2m^2}\Gamma(0, m^2R^2) - \ln(\tfrac{1}{2}m\xi)] \times[1 + O(\xi^2)]\}, \tag{3.6}$$

where $\gamma = 0.577\,215\cdots$ is Euler's constant and $\Gamma(a, x)$ is an incomplete gamma function.[30] In obtaining (3.5), we have taken advantage of the fact that μ^2 is small and used a small-x approximation for $\Gamma(0, \mu^2R^2)$.

A. Solution of Temperature Equation

Since the proton and pion systems are treated asymmetrically in the temperature equation, it is convenient to break (3.4) into two coupled equations which are, in the high-energy limit,

$$\frac{2}{\xi[D - \ln(\frac{1}{2}m\xi)]} = E_p = (1-\eta)\sqrt{s}, \tag{3.7}$$

$$\frac{G}{\alpha} + \frac{1}{2\alpha[\frac{1}{2}\gamma + \ln(\alpha/2R)]} = E_\pi = \eta\sqrt{s}. \tag{3.8}$$

In (3.7),

$$\xi = \alpha - \frac{2\lambda}{\sqrt{s}} \quad \text{and} \quad D = -[\gamma + \tfrac{1}{2}e^{R^2m^2}\Gamma(0, R^2m^2)],$$

and in (3.8),

$$G = \pi R^{-2}[z_0 + 2(z_+z_-)^{1/2}].$$

To obtain (3.8), we have used the asymptotic expansion of $I_1(x)/I_0(x)$. A zeroth-order solution to the proton equation (3.7) is

$$\xi^{(0)} = \frac{2}{E_p(r_p + \ln r_p)}, \tag{3.9}$$

where $r_p = D + \ln(E_p/m)$. The next-order correction in a Newton-Ralphson approximation is[35]

$$\xi^{(1)} - \xi^{(0)} \cong -2(\ln r_p)/(E_p r_p^3). \tag{3.10}$$

To leading order in powers of logarithms, the proton contribution to $Q(\beta)$ is

$$\psi_N(\xi^{(0)}) = \frac{\pi}{R^2}(r_p + \ln r_p). \tag{3.11}$$

A zeroth-order solution to the pion equation (3.8) is given by

$$\beta^{(0)} = \frac{G}{E_\pi}\left(1 - \frac{1}{2Gr_\pi}\right), \tag{3.12}$$

where

$$r_\pi = \left(-\tfrac{1}{2}\gamma + \ln\frac{2RE_\pi}{G}\right).$$

The next-order correction in a Newton-Ralphson approximation is given by

$$\beta^{(1)} - \beta^{(0)} \cong (4GE_\pi r_\pi^3)^{-1}. \tag{3.13}$$

The pion contribution to $Q(\beta)$ is then given approximately by

$$\varphi_\pi(\beta^{(0)}) \approx \frac{\pi}{R^2}[r_\pi + (2Gr_\pi)^{-1}]. \tag{3.14}$$

To obtain the subsidiary quantities necessary for computing Ω, we first equate the pion solution $\beta^{(0)} - 2\lambda/\sqrt{s}$ from (3.12) with the proton solution $\xi^{(0)}$ from (3.9), obtaining

$$r_p \cong D + \ln[(1 - G/2\lambda)\sqrt{s}/m], \tag{3.15}$$

$$r_\pi \cong -\tfrac{1}{2}\gamma + \ln(R\sqrt{s}/\lambda) \tag{3.16}$$

for $G/(2\lambda) < 1$. The high-energy behavior of the inelasticity is then given by

$$\eta(s) \cong \left(\frac{G}{2\lambda}\right)\left(1 - \frac{2}{(2\lambda - G)r_p} - \frac{1}{2Gr_\pi}\right), \tag{3.17}$$

while from (3.11) and (3.14), the grand partition function is

$$Q(\beta) = \frac{R}{2\pi(z_+z_-)^{1/4}r_\pi^{1/2}}[(\pi/R^2)(r_p + \ln r_p)]^2\exp(Gr_\pi) \times\left[1 + \left(\tfrac{1}{2} + \frac{R^2}{16\pi(z_+z_-)^{1/2}}\right)\Big/ r_\pi + \cdots\right]. \tag{3.18}$$

Using the equations analogous to (2.20)–(2.22) in this limit, the $\det B$ correction terms are

$$B_{00} = \tfrac{1}{2}s(1 - G/2\lambda)^2(r_p + \ln r_p), \tag{3.19}$$

$$B_{LL} = \left(\frac{s}{2\lambda}\right)\left(1 - \frac{2}{2\lambda - G}\Big/ r_p\right), \tag{3.20}$$

$$B_{TT} = (1/2R^2)[Gr_\pi + (3 - G)/2]. \tag{3.21}$$

B. Total Rate and Inclusive Moments

We get the total inelastic rate using an equation analogous to (2.23). To leading powers in logarithms of the energy the result is

$$\Omega^{(0)} \sim \frac{s^{\delta+G/2-1} R^{G-1} \lambda^{1/2-G} \exp(2\lambda - \gamma G/2)}{2\pi G (z_+ z_-)^{1/4}(1 - G/2\lambda)} \times \left(\frac{r_p + \ln r_p}{r_\pi}\right)^{3/2} \left[1 + O\left(\frac{\ln r_p}{r_p}\right) + O\left(\frac{1}{r_\pi}\right)\right]. \quad (3.22)$$

The flux factor which relates the total inelastic rate to the total inelastic cross section behaves asymptotically as s^{-1} so that the condition that the total inelastic cross section be asymptotically constant within logarithms is

$$\delta = 2 - G/2 . \quad (3.23)$$

Taking this value for δ satisfies our assumption (4) in Sec. II.

Given the asymptotic expression (3.22) for the total inelastic rate, there are several average quantities which can be calculated directly from this rate by differentiation. For example, the multiplicity moments for producing π^- are defined by

$$f_k = z_-^{\,k} \frac{\partial^k}{\partial z_-^{\,k}} \ln\Omega . \quad (3.24)$$

From (3.18)–(3.21), we get

$$f_k = A_k \ln s + B_k + O(1/\ln s) , \quad (3.25)$$

$$A_k = (-)^{k+1} (\pi/2R^2)(z_+ z_-)^{1/2} \Gamma(k - \tfrac{1}{2})/\Gamma(\tfrac{1}{2}) . \quad (3.26)$$

Of particular interest for our later discussion is the behavior of f_1 and f_2. From (3.25) we see that asymptotically

$$\frac{f_2}{f_1} = \frac{\langle n_-(n_- - 1)\rangle - \langle n_-\rangle^2}{\langle n_-\rangle} \underset{s\to\infty}{\sim} -\tfrac{1}{2} . \quad (3.27)$$

The presence of weak negative correlations of this type due to charge conservation has been derived before in the context of a multiperipheral model.[36,37]

In addition to the f_k and the average inelasticity [Eq. (3.17)], it is of interest to compute the average transverse momentum of a pion. For convenience in obtaining an analytic solution, we calculate

$$\langle q_T^{\,2}\rangle = -\frac{1}{\langle n_\pi\rangle} \frac{\partial}{\partial R_\pi^{\,2}} \ln\Omega . \quad (3.28)$$

In order to obtain this result by differentiation, we have distinguished between the cutoff parameter R^2 for pions and protons. The average is, using (3.18)–(3.21),

$$\langle q_T^{\,2}\rangle \cong \frac{1}{R^2}\left(1 - \frac{1 + 2/G}{\ln(sR^2/\lambda^2)}\right). \quad (3.29)$$

We give the results of the numerical calculations for $\langle \eta\rangle$, f_1, f_2, and $\langle q_T\rangle$ in Sec. IV.

C. Inclusive Spectra

As discussed in Sec. II, the leading-particle effect is responsible for the differences in shapes of the nucleon and pion inclusive spectra. To illustrate the problem of extracting an inclusive distribution from the model analytically, consider the high-energy-limit analog of Eq. (2.26) in the grand partition function

$$2\left[\frac{\xi^2 + \lambda^2 x^2/M_L^{\,2}}{\xi^2}\right]^{1/2} \Big/ \xi\left[D - \ln\frac{m\xi}{2}\right] + \frac{G}{\alpha}\Big|_{\alpha=\beta'} = M_L . \quad (3.30)$$

Here ξ and M_L are given by (2.25) and (2.27), respectively. The boost u which relates the c.m. frame to the frame where the unobserved particles have no longitudinal momentum is given by

$$\sinh u = q_L/M_L = x s^{1/2}/2M_L . \quad (3.31)$$

It is clear that the value of β' depends upon the relative size of ξ and

$$\frac{2\lambda}{\sqrt{s}} \sinh u = \frac{\lambda x}{M_L} .$$

When $\xi \gg \lambda|x|/M_L$ we have a solution to (3.30),

$$\beta' = (2\lambda/M_L)(1 - \omega/s^{1/2}) + O(1/M_L \ln M_L) \approx 2\lambda/s^{1/2} . \quad (3.32)$$

We term this the *isothermal* solution and the region in x in which it holds the *isothermal region*. In this region, the one-particle distribution has the behavior

$$\rho^\pi(x, q_T^{\,2}) \approx \exp\left[-\left(R^2 + \frac{1}{2B_{TT}}\right) q_T^{\,2} - \lambda x\right], \quad (3.33)$$

using (3.22) to calculate Ω and $d\Omega/(d^3q/\omega)$.

The size of the isothermal region where (3.33) is approximately valid shrinks logarithmically with increasing energy. This is because for fixed x and $s \to \infty$, the solution for ξ given by (3.30) is

$$\xi \cong \frac{2}{M_L}\left\{\frac{\lambda|x|}{1 - G/2\lambda} \Big/ \ln\left[\frac{M_L^{\,2}}{m^2\lambda|x|}(1 - G/2\lambda)\right]\right\}^{1/2} \quad (3.34)$$

so that the condition

$$\xi > \frac{\lambda|x|}{M_L} \quad (3.35)$$

cannot hold for a given x independent of energy. We see that the form (3.33) does not scale in x. However, the shrinkage of the isothermal region is quite slow, and extends for

$$|x| \lesssim \tfrac{1}{4}$$

at CERN Intersecting Storage Ring (ISR) energies ($\sqrt{s} \approx 100$ GeV) with the parameter λ chosen to be

5.

For x near 1, the condition that ξ be greater than zero gives another limiting solution to (3.30),

$$\beta' \cong \frac{2\lambda}{M_L} . \tag{3.36}$$

In this limit,

$$\rho_\pi(x, q_T^2) \cong (1 - |x|) \exp\left[-\left(R^2 + \frac{1}{2B_{TT}}\right) q_T^2\right], \tag{3.37}$$

where the condition (3.23), which gives a constant total inelastic cross section, ensures that the exponent of $(1 - |x|)$ is unity. Without this condition, we would have a different x behavior for the inclusive distributions.

The one-proton distribution can be extracted in an analogous way. Because of (2.4), which guarantees that each proton emerges on the average with a large fraction of the energy, there is no isothermal region for a proton distribution. Thus, relative to the exponential x behavior of the pion distribution, the proton distribution is flat for $x \lesssim 0.2$–0.4.

Two-particle inclusive distributions involve one new feature, the dependence on transverse angle, which can be handled analytically in our model. This is because the $\alpha_T \to 0$ limit in (2.14) and (2.15) leaves only a simple Gaussian dependence on the transverse momentum of the missing particles in (2.23). For a two-particle distribution, we then have

$$\rho_2(x_1, q_{1T}^2; x_2, q_{2T}^2; \varphi) \propto \exp\left\{-\frac{q_{1T} q_{2T}}{B_{TT}} \cos\varphi\right\}, \tag{3.38}$$

where B_{TT}, as given by (2.22), is an implicit function of x_1, x_2 through the temperature equation. For x_1, x_2 both near 1, Eq. (3.21) gives

$$B_{TT} \cong \frac{1}{2R^2}\left[G\left(-\tfrac{1}{2}\gamma + \ln\frac{R\sqrt{s}}{\lambda} + \tfrac{1}{2}\ln\frac{M_L^2}{s}\right) + \frac{3}{2} - \frac{G}{2}\right], \tag{3.39}$$

where

$$\frac{M_L^2}{s} \cong \begin{cases} 1 - |x_1| - |x_2| & \text{for } x_1 x_2 > 0 \\ (1 - |x_1|)(1 - |x_2|) & \text{for } x_1 x_2 < 0 \end{cases} \tag{3.40}$$

so that the transverse angle dependence of ρ_2 vanishes for fixed $|x_1|$ and $|x_2|$ near 1 as $\sqrt{s} \to \infty$.

IV. NUMERICAL RESULTS AND COMPARISON WITH DATA

This section presents specific numerical calculations based on the model described in Sec. II. These numerical results are compared both with our expectations based on the analytic solution to the high-energy limit and, where appropriate, with available data. The goal is to present the two-particle inclusive spectrum for $pp \to \pi^-\pi^- X$ at $P_{\text{lab}} = 21$ GeV/c. In addition, since we are employing in the numerical calculations a microscopic model, we present several other quantities which test the reasonableness of our input and give some insight into the exclusive processes from which the inclusive quantities are constructed.

A. Determination of the Parameters

In order to make numerical calculations with Eq. (2.7), we must specify the values of the four parameters it contains. The quantity δ is fixed according to assumption (4) in Sec. II. The parameter R^2 determines the range of cutoff of the transverse momenta. From analytic considerations based on the high-energy limit of the model, this parameter determines the large-q_T^2 behavior of the single-pion inclusive spectrum in the central region. For q_T^2 large compared with $\langle q_T^2 \rangle$, $x = (2\kappa_\pi/\sqrt{s}) \sinh y$ is near unity and solution (3.37) applies. For y fixed,

$$\rho^\pi(y, q_T^2) \propto e^{-R^2 q_T^2}, \tag{4.1}$$

where y is the pion rapidity, $y = \sinh^{-1}(q_L/\kappa_\pi)$. As our initial choice, we take

$$R^2 = 4 \text{ (GeV/}c\text{)}^{-2}. \tag{4.2}$$

For simplicity, we choose the cutoff in the nucleon transverse momentum to be the same as that for the pions.

In the high-energy limit, as shown in (3.33), the parameter λ which ensures the small inelasticity of the final nucleons is approximately the slope of the one-pion distribution plotted against the Feynman scaling parameter x,

$$\rho^\pi(x, q_T^2)|_{\text{small } x} \simeq e^{-\lambda|x|} . \tag{4.3}$$

Our initial choice of $\lambda = 5$ is taken to match the experimental value of this slope.[38]

The final parameter, z, the coupling constant for producing a pion, determines the relative normalization of the phase-space integrals for producing n and $n+1$ pions. Since our primary purpose is to discuss inclusive spectra at $P_{\text{lab}} = 21$ GeV/c, z is adjusted to fit the experimental value of the average number of π^- per inelastic pp collision,[2,39]

$$\langle n_- \rangle_{\text{exp}} = 1.08 \pm 0.04 . \tag{4.4}$$

This guarantees that the normalization of the one-particle distribution is correct at one energy. With R^2 and λ fixed as above, (4.4) requires that z be 3.70 GeV^{-2}. Computing $\langle n_- \rangle$ with these parame-

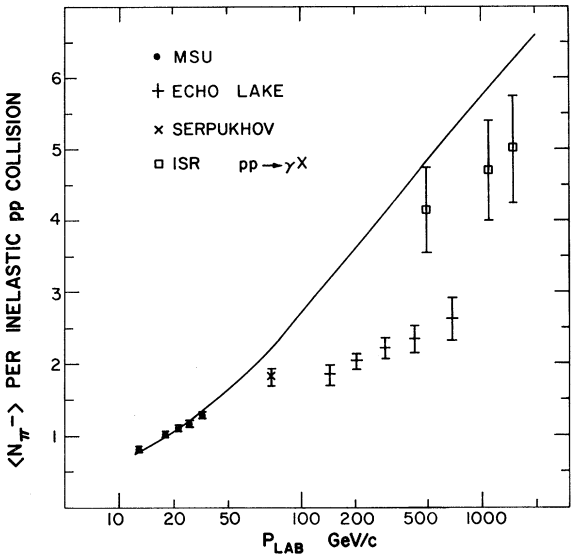

FIG. 1. The IEM predictions for average number of negative pions per inelastic pp collision as a function of laboratory momentum, using the parameters $R^2=4$ $(\mathrm{GeV}/c)^{-2}$, $\lambda=5$, and $z=3.70$ GeV^{-2}. The energy parameter δ is -0.3. The data are from Refs. 2 and 39–43. Unless otherwise specified, the curves in all figures are calculated from the IEM with the same choice of parameters as here.

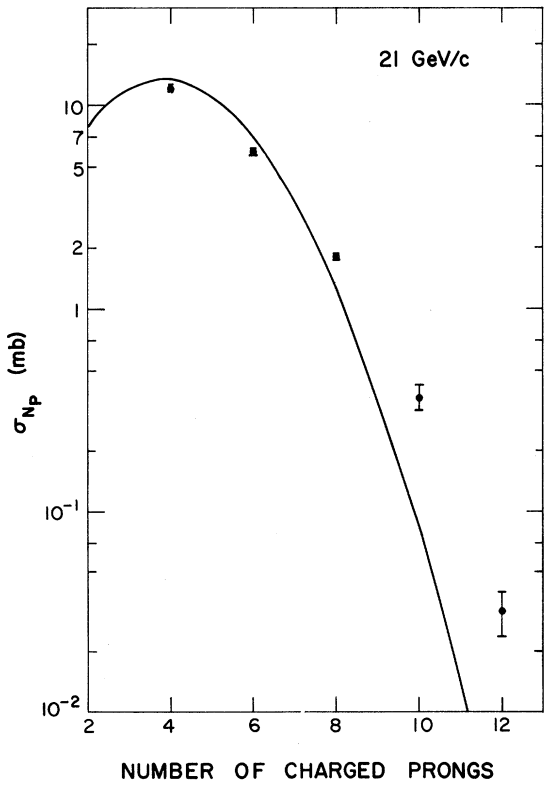

FIG. 2. Inelastic charged prong cross sections at $P_{\mathrm{lab}}=21$ GeV/c, compared with data (Ref. 39).

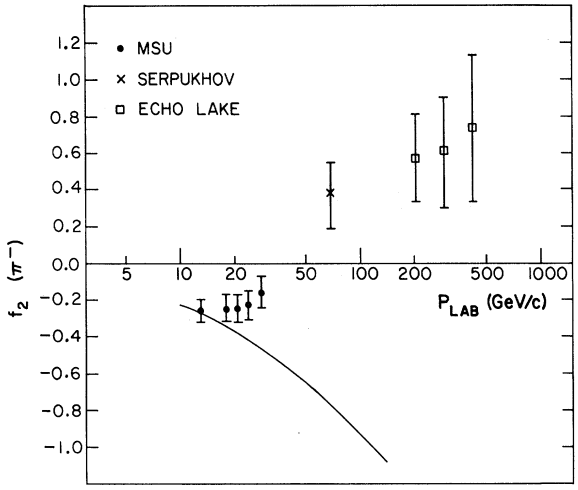

FIG. 3. Behavior of $f_2=\langle n_-(n_--1)\rangle-\langle n_-\rangle^2$ as a function of energy, compared with data (Refs. 2, 41, and 42).

ters at other lab momenta[40-43] (Fig. 1), we note some disagreement. We shall return to this point later, noting here that the difficulty may be related to underestimating the low-prong-number cross sections due to the lack of diffraction components in the model.

B. Inclusive and Exclusive Moments

The functions $\psi(\xi)$ and $\varphi(\alpha)$ [given by (2.14) and (2.15)] and their derivatives are calculated by Gaussian integration for $\alpha_T=0$. The solution to the temperature Eq. (2.19) for each value of the number of pions is obtained numerically using the Newton-Ralphson method.[35] The approximation to the phase-space integrations given by (2.23) is used, ignoring the higher-order corrections terms $\mathfrak{R}(\beta,P_T)$. Then, using the Cerulus isospin weights given by (2.6), the prong-number cross sections are calculated.

Figure 2 shows the comparison of the model with the prong-number cross sections at 21 GeV/c. The mean value is used as input, but the higher moments are predictions. For example, the second moment,

$$\langle n_\pi(n_\pi-1)\rangle=0.79\,, \tag{4.5}$$

can be compared with the experimental value 0.92 ± 0.04. This reflects a general tendency of many statistical models to predict multiplicity distributions narrower than the data.[37] The quantitative measure of this is $f_2^-=\langle n_-(n_--1)\rangle-\langle n_-\rangle^2$, which is also the value of the integrated $\pi^-\pi^-$ correlation function. Experimentally $f_2=-0.24\pm0.08$, whereas (4.5) gives $f_2=-0.38$. At higher energies, the discrepancy becomes significant (Fig. 3) suggesting

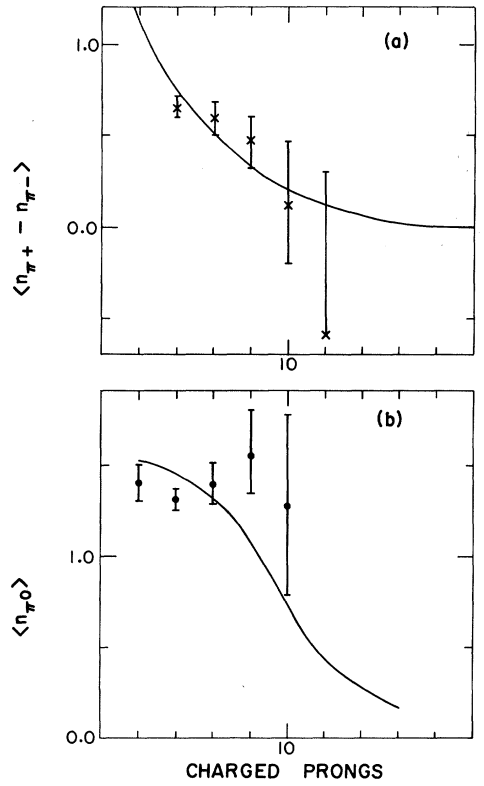

FIG. 4. (a) The surplus of π^+ over π^- as a function of prong number at 21 GeV/c, compared with data (Ref. 39). (b) The number of π^0 as a function of prong number. Curve is prediction of model at 21 GeV/c; data are at 19 GeV/c (Ref. 40).

that important dynamic features are missing in this description. For example, diffractive dissociation components in the production cross sections would imply that asymptotically $f_2 > 0$.[44] There is no diffraction in the independent emission model either in the elastic or the production cross sections. One of the reasons we normalize inclusive quantities to the total inelastic cross section instead of the total cross section in the model is that the rapid falloff of our elastic cross section (see Appendix) is in drastic disagreement with experiment. At low energies, the error in omitting diffractive mechanisms in production might be small, but at higher energies they are bound to be important.[7]

It is important for comparison with inclusive data that our treatment of isospin be reasonable. With the number of π^-'s fixed by (4.4), we predict the average number of π^+'s and π^0's at 21 GeV/c to be

$$\langle n_+ \rangle = 1.87\,, \qquad \langle n_0 \rangle = 1.42\,. \tag{4.6}$$

The average number of π^+'s and π^0's per charged

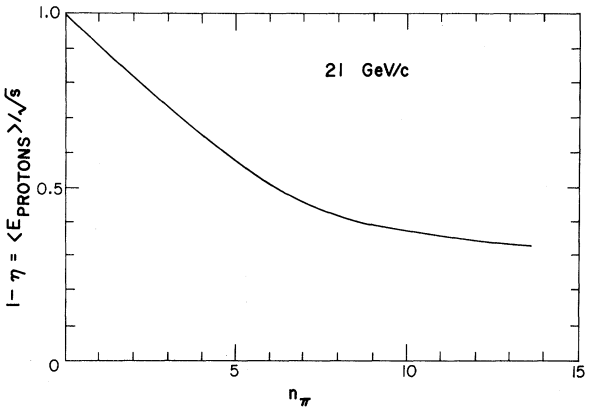

FIG. 5. Elasticity, defined as energy of final-state nucleons divided by initial energy, as a function of number of final-state pions.

prong (Fig. 4) is in reasonable agreement with experiment, but we note that such agreement does not guarantee that our assumptions concerning the treatment of isospin are correct. Controversy in the literature concerning Fermi's isospin weights involves detailed comparison of specific final states[45] while we are only assuming that the approximations are adequate for treating inclusive and semi-inclusive measurements.

Two quantities which directly test our dynamic input are the average inelasticity of the protons and the average transverse momenta of the pions. The average energy of the protons for each number of pions (Fig. 5) is calculated by solving (2.19) and evaluating

$$\langle 1-\eta_n \rangle = \langle E_p \rangle_n s^{-1/2} = -2s^{-1/2} \frac{\partial}{\partial \beta} \ln \psi_N\,. \tag{4.7}$$

Summing over the produced pions, the average in-

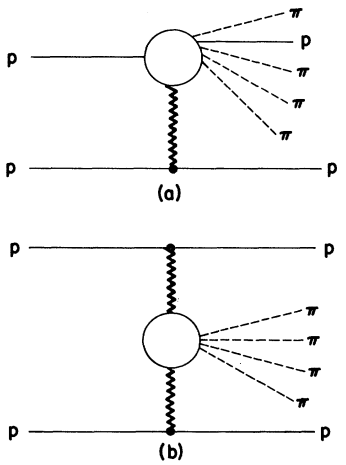

FIG. 6. (a) Fragmentation or excitation picture. (b) Pionization picture.

elasticity is

$$\langle \eta \rangle = 1 - \frac{\sum_n \sigma_n \langle E_p \rangle_n s^{-1/2}}{\sum_n \sigma_n} = 0.37 . \quad (4.8)$$

We note that, for n small, the average inelasticity per pion is approximately constant,[26]

$$\frac{\eta_n}{n} \cong \frac{\eta}{\langle n \rangle} \cong \frac{1}{\lambda \ln s} . \quad (4.9)$$

This consequence of the way in which we have incorporated the leading particle effect is roughly what one would expect from a picture [Fig. 6(a)] where the pions compete with at least one of the final-state nucleons for the available energy. In contrast, Fig. 6(b) depicts a situation in which the momentum transfer between an initial and final nucleon is roughly independent of the number of pions. The pions then compete only with each other for the available energy. This would be the case if all the pions were emitted from the center of a multiperipheral chain. Previous calculations involving statistical models have relied heavily on Fig. 6(b).[14,15,46,47] At least at currently available energies, it seems that this situation conflicts with data.

The average value of transverse momentum of a pion in an n-pion final state (Fig. 7) is approximately

$$\langle q_T \rangle_n = \frac{\int_0^\infty dq_T{}^2 \, q_T \, e^{-R^2 q_T{}^2} K_0(\beta_n(\mu^2 + q_T{}^2)^{1/2})}{\int_0^\infty dq_T{}^2 \, e^{-R^2 q_T{}^2} K_0(\beta_n(\mu^2 + q_T{}^2)^{1/2})} , \quad (4.10)$$

where β_n is given by (2.16). The average pion transverse momentum predicted by the model at 21 GeV/c is 0.316 GeV/c compared to the experimental value 0.309 ± 0.005. The fact that (4.10) gives a much smaller value for $\langle q_T \rangle$ than what one would expect asymptotically from the form $e^{-4q_T{}^2}$ ($\approx$0.45 GeV/c; see Sec. III) indicates to us the importance of nonasymptotic contributions at 21 GeV/c. Notice that, using the δ function in (2.5), the factors involving λ in the integrand can be rewritten using pion energies,

$$\prod_{i=1}^{2} \exp(2\lambda E_i s^{-1/2}) \delta\left(\sqrt{s} - E_1 - E_2 - \sum_{j=1}^{n} \omega_j\right) = e^{2\lambda} \prod_{j=1}^{n} \exp(-2\lambda \omega_j s^{-1/2}) \delta\left(\sqrt{s} - E_1 - E_2 - \sum_{j=1}^{n} \omega_j\right) . \quad (4.11)$$

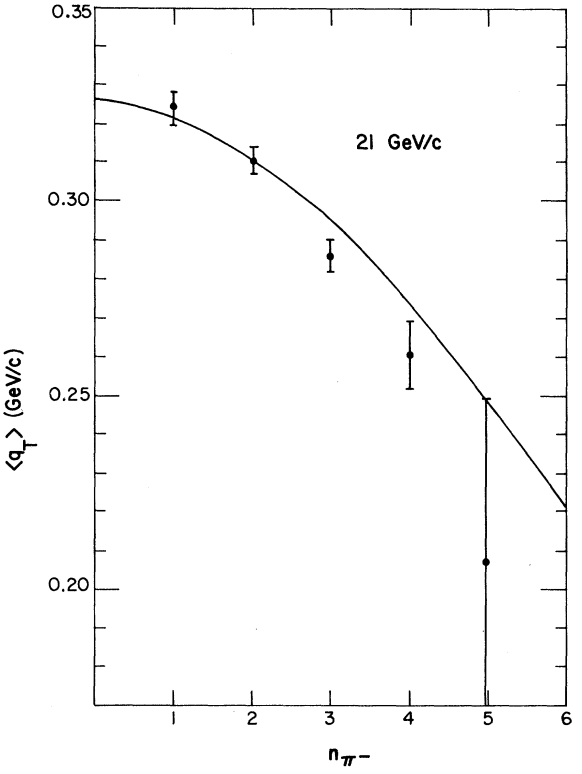

FIG. 7. Average pion transverse momentum as a function of number of π^-'s in the final state at 21 GeV/c, compared with data (Ref. 39).

At $P_{\text{lab}} = 21$ GeV/c, $2\lambda s^{-1/2} \cong 1.56$ and the damping in pion energies provides a substantial extra damping in transverse momentum. The s dependence of $\langle q_T \rangle$ in Fig. 8 indicates that the predicted shape of the transverse-momentum distribution will change substantially by ISR energies.[48] From these considerations it seems that experimental evidence on the value $\langle q_T \rangle$ at ISR indicate important dynamic effects not present in our model.

C. The π^- Inclusive Spectra

To calculate the inclusive π^- distributions (2.8), we proceed as in the calculation of the rate. The π^- distribution is given by

$$\rho^-(s, y, q_T{}^2) = \Omega^{-1} e^{-R^2 q_T{}^2} \sum_{n=1}^{\infty} \frac{z^n}{n!} \left[\sum_{n_+ + n_- + n_0 = n} n_- W(n_+, n_-, n_0) \right] d\Omega_n \Big/ \frac{d^3q}{\omega} . \quad (4.12)$$

Here, the phase-space integral $d\Omega_n/(d^3q/\omega)$ is evaluated at a total four-momentum $P - q$, which will have a zero longitudinal component in a frame other than the c.m. frame. The discussion of how to calculate such integrals is given in Sec. II. The π^- x distribution is given in Fig. 9; for compari-

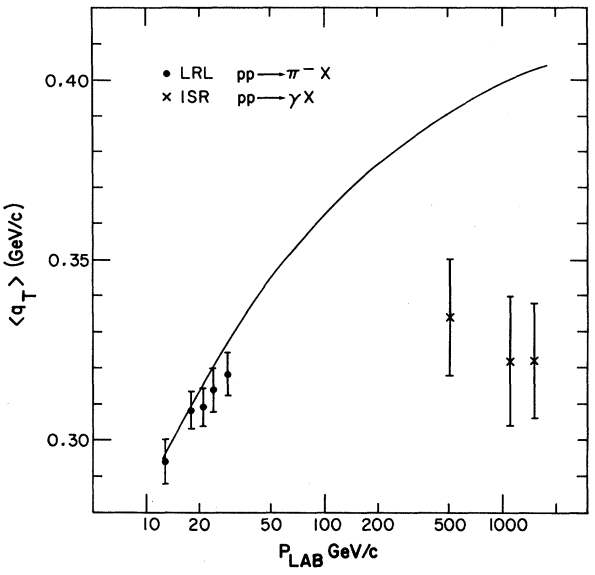

FIG. 8. Average pion transverse momentum as a function of lab momentum, compared with data (Refs. 39 and 48).

son, the proton x distribution is also given. We note that the results agree with our expectations based upon the asymptotic solution. In Fig. 10, we show the π^- transverse-momentum distribution. Here, we see a nonasymptotic behavior contributing a sharp forward peak, due to the way we have introduced small inelasticity. At present, we would not like to associate this peak with the observed sharp peak in the data, since the latter scales in the range $20 \leq p_{\text{lab}} \lesssim 1000$ GeV/c, whereas the one in our model does not.[49]

Now that we have checked that the model correctly reproduces the features expected from the asymptotic calculation, we next check the model against experimental distributions. In Fig. 11, we compare the π^- rapidity distribution with the 21-GeV/c data, and note that the agreement is quite good. This agreement indicates that we have correctly implemented our starting assumptions.

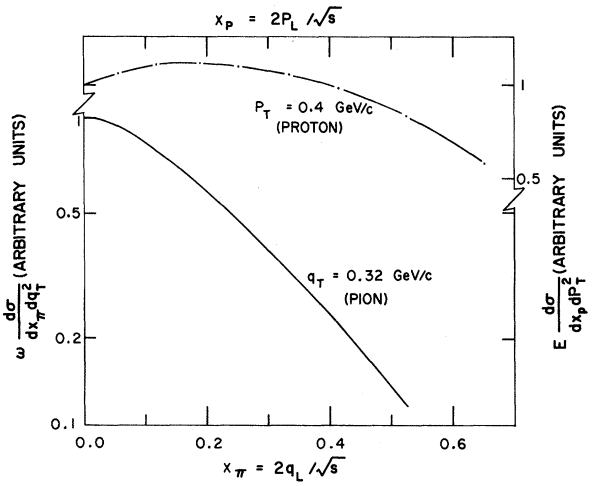

FIG. 9. Comparison of proton and pion x distributions in the model at 21 GeV/c.

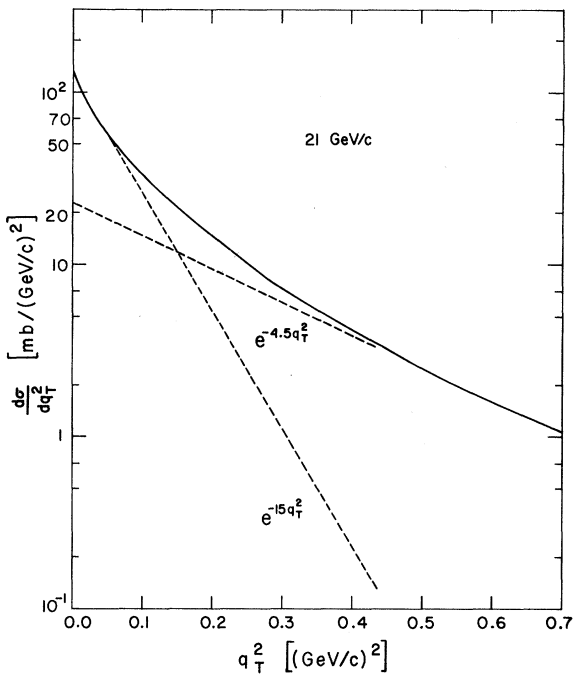

FIG. 10. Transverse-momentum distribution for a π^- at 21 GeV/c in the model.

The $\pi^-\pi^-$ distributions $\rho_2^-(y_1, y_2)$ are given in Fig. 12. Comparing our description with the nova-model predictions for the same data, we find similar results. One discrepancy is the over-all normalization, equal to $\langle n_-(n_- - 1)\rangle$, which, as discussed above, is underestimated due to possible neglect of diffractive contributions. Another discrepancy is a noticeable trend of the IEM to predict an excess of events for $y_2 > 0$ when $y_1 \gtrsim 0.8$. Also, our curves have roughly the same width for different values of y_1, whereas the data become broader for $y_1 > 1.2$. We conclude that there may be interesting dynamic effects here which have not been included in the model, although the gross features of the data are certainly explained.

From $\rho_2^-(y_1, y_2)$ and $\rho^-(y)$ we can go on to calculate the correlation function

$$C_2(y_1, y_2) = \rho_2^-(y_1, y_2) - \rho^-(y_1)\rho^-(y_2), \qquad (4.13)$$

as shown in Fig. 13. This is chiefly interesting in the IEM in that the asymmetry in $\rho_2^-(y_1, y_2)$ shows up as a ridge along $y_1 \approx y_2$ in the correlation function. The data also show a ridge but with a positive correlation. The failure of the IEM to give a positive correlation can be understood by noting

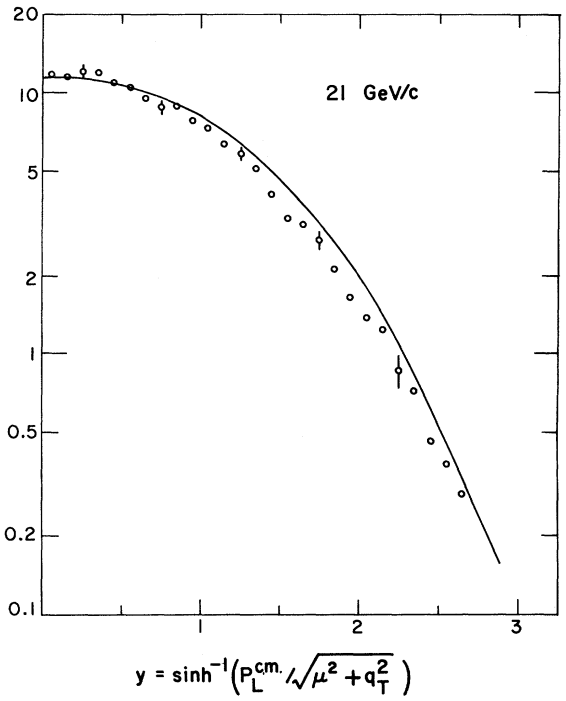

FIG. 11. Rapidity distribution for a π^- at 21 GeV/c in the model, compared with data (Ref. 2). The vertical scale is $d\sigma/dy$ in units of mb.

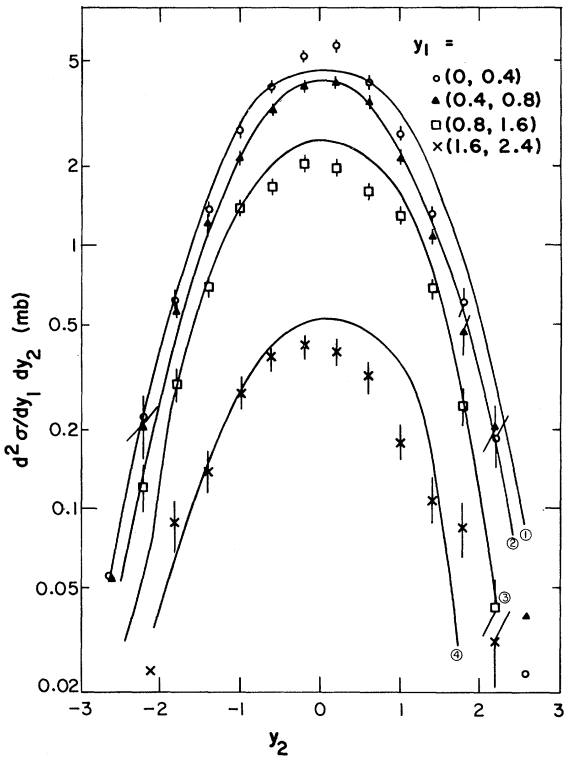

FIG. 12. Two-particle inclusive distribution $pp \to \pi^-\pi^- X$ as a function of rapidity y_2 at 21 GeV/c. Curves (1), (2), (3), and (4) are at rapidity $y_1 = 0.2$, 0.6, 1.2, and 2.0, respectively. Data are from Ref. 2.

once again that we underestimate the normalization of $\rho_2^-(y_1, y_2)$.

V. CONCLUSIONS

With the aid of the independent emission model, we have examined the implications for inclusive spectra of the following.

(1) conservation laws.
(2) small transverse momenta.
(3) small average inelasticity.
(4) constant total inelastic cross section.

We find these assumptions adequate to reproduce a large portion of the available data, but there are indications for the necessity of additional dynamic input.

The behavior of $f_2 = \langle n_-(n_- - 1)\rangle - \langle n_-\rangle^2$ as a function of s predicted by the model is in conflict with available experimental data. The simplest way of reconciling this discrepancy is to hypothesize the presence of diffractive components[7] for at least some production cross sections although other ways of introducing extra dynamic correlations must be considered as well.

The observed experimental energy independence from Zero-Gradient Synchrotron (ZGS) to ISR energies of $\langle q_T\rangle$ and the shape of the pion transverse-momentum spectrum are not simple consequences of the way in which implications (1)–(4) are implemented in the model. Even though the predicted $\langle n_\pi\rangle$ is approximately a linear function of ln$s$ for $P_{\text{lab}} \gtrsim 20$ GeV/c, it is not true that all quantities in the model rapidly assume their asymptotic behavior.[47] There seems to be some important information in the early achievement of scaling which indicates the presence of complicated rather than simple dynamics.

We have shown, in contrast to other claims,[27] that

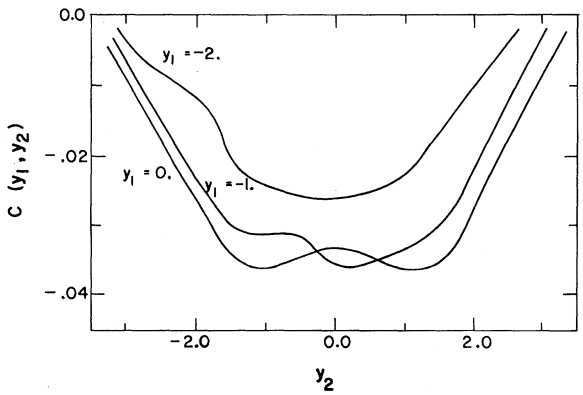

FIG. 13. Predicted two-particle correlation function at 21 GeV/c.

scaling in x is not a direct consequence of (1)–(4). We do have scaling in y and a quasiscaling in x where the scaling region shrinks very slowly with s. This quasiscaling may be experimentally indistinguishable from actual scaling.

Details in the shape of π rapidity spectra are sensitive to the way in which (3) is enforced. The statistically unbiased way to introduce a small "average" inelasticity is to have a proton distribution which is flat in x. A flat proton distribution emerges naturally from a "fragmentation" rather than a "pionization" picture, and our π distributions are similar to those found in models which can be pictured as in Fig. 6(a)[1,21,22] rather than in models pictured as in Fig. 6(b).[14,15,46,47] We emphasize here that the data at low energies definitely are better reproduced in a fragmentation picture.

Finally, we conclude that the observed experimental shape of the two-particle inclusive spectra indicates the possibility of additional dynamic features not contained in assumptions (1)–(4).

ACKNOWLEDGMENTS

We are indebted to Dr. Richard Arnold and Dr. Edmond Berger for many valuable comments and innumerable conversations concerning this work.

APPENDIX: THE ERRORS IN THE APPROXIMATION METHOD AND THE ELASTIC SCATTERING CONTRIBUTION

It is important to understand the kind of errors that the approximation of steepest descents introduces into the inverse Laplace transform. Lurçat and Mazur[24] show that, at a given energy, the method produces an asymptotic expansion valid when the number of particles is large. They also discussed in great detail the magnitude of the errors both with and without correction terms when the method is applied to pure phase-space integrals and concluded that the method provides a good approximation for $n \gtrsim 5$ independent of energy.

The usefulness of the method of steepest descents obviously depends on the type of matrix element, so we cannot accept the LM conclusions in our case without further examination. Although it is not appropriate to go into a detailed error analysis, it is instructive to consider the integral for elastic scattering with our matrix element. The integral can be evaluated exactly and compared directly with the approximate result. The integral to be evaluated is

$$\Omega_2 = \int \frac{d^3p_1}{2E_1}\,\frac{d^3p_2}{2E_2}\, e^{-R^2(p_{1T}^2 + p_{2T}^2)} \times \delta(\sqrt{s} - E_1 - E_2)\,\delta^{(3)}(\vec{p}_1 + \vec{p}_2)$$
$$= \frac{\pi p}{2s^{1/2}} \int_{-1}^{+1} d(\cos\theta)\, e^{-2R^2 p^2 \sin^2\theta}\,. \tag{A1}$$

The remaining integral is expressible in terms of an error function[30]:

$$\Omega_2 = \left(\frac{\pi}{2}\right)^{3/2} s^{-1/2}\, \frac{e^{-2R^2p^2}}{iR}\, \mathrm{erf}(i\sqrt{2}\,Rp)\,. \tag{A2}$$

In order to compare this exact result with our approximate solution, we use the asymptotic form

$$\mathrm{erf}(ia) \underset{a\to\infty}{\sim} i\pi^{-1/2} a^{-1} \exp(a^2) \times \left(1 + \frac{2!}{1!(2a)^2} + \frac{4!}{2!(2a)^4} + \cdots\right) \tag{A3}$$

so that

$$\Omega_2 \cong \frac{\pi}{4R^2 p\sqrt{s}} \left(1 + \frac{1}{4R^2p^2} + \frac{3}{16R^4p^4} + \cdots\right). \tag{A4}$$

We now compare this with the estimate obtained from the high-energy solution to the LM approximation. In the usual way, we first solve the temperature equation, and then evaluate $\Phi_2(\beta) = \psi_N{}^2$ and $\det B$. To leading order as $s \to \infty$, the results are

$$\beta \simeq \frac{2}{\sqrt{s}}\,\frac{1}{r + \ln r}\,,$$
$$\Phi_2 = \left[\left(\frac{\pi}{R^2}\right)(r + \ln r)\right]^2,$$
$$B_{00} = \tfrac{1}{2}s(r + \ln r)\,, \tag{A5}$$
$$B_{LL} = \tfrac{1}{2}s(r + \ln r)\,,$$
$$B_{TT} = 1/R^2\,,$$

where $r = D + \ln(\sqrt{s}/m)$ (see Sec. III). To zeroth order [ignoring $\mathfrak{R}(\beta, P_T = 0)$ in (2.23)], the LM approximation is

$$\Omega_2^{\mathrm{LM}} \cong (1/2R^2 s)(r + \ln r) \tag{A6}$$

in the high-energy limit.

Thus, we find that the ratio between the approximation and the exact solution,

$$\frac{\Omega_2^{\mathrm{LM}}}{\Omega_2} \cong \frac{1}{\pi}(r + \ln r)\,, \tag{A7}$$

increases logarithmically as $s \to \infty$. In contrast, for pure phase space ($R^2 = 0$), the ratio varies between 2.4 and 2.2 between threshold and $s \to \infty$.

In calculating inclusive quantities with our model, we normalized to the inelastic cross section and not the total cross section so the error in the elastic cross section is not, by itself, important. It does, however, provide a strong clue that we may

be making the same type of errors in evaluating other cross sections for low numbers of pions. Of course, for sufficiently large numbers of pions, we expect the errors to be of order $1/\sqrt{n}$, at a fixed energy. However, since we do not know at which n the errors in fact start to decrease, it remains an interesting and open problem to estimate the errors in calculating the inelastic total rate as well as other inclusive quantities. A clue to this problem may be obtained by evaluating the next higher term, $\mathcal{R}(\beta, P_T)$, in (2.23). A complete error analysis for production cross sections in this scheme, utilizing comparisons with Monte Carlo techniques, is in progress.

The justification for truncating the asymptotic expansion at the first term in our calculations is that it seems probable that these errors essentially produce an uncertainty in the parameters z and δ in (2.7). The value of z determines the relative normalization of cross sections producing different numbers of pions and this value is chosen to fit the observed number of pions. An n-dependent bias in evaluating the integrals then, to a good approximation, just changes the value of z we use. Similarly, logarithmic energy dependence of the cross sections is unimportant compared to the energy dependence produced by a numerical indeterminacy in δ.

---

*Work performed under the auspices of the U. S. Atomic Energy Commission.

[1]E. L. Berger and M. Jacob, this issue, Phys. Rev. D 6, 1930 (1972).

[2]E. L. Berger, B. Y. Oh, and G. A. Smith, Phys. Rev. Letters 29, 675 (1972).

[3]A. Białas, K. Fiałkowski, R. Wit, and K. Zalewski, Phys. Letters 39B, 211 (1972).

[4]See also several of the references below, in particular Refs. 37 and 46.

[5]E. Fermi, Progr. Theoret. Phys. (Kyoto) 5, 570 (1950); Phys. Rev. 92, 452 (1953); 93, 1434 (1954).

[6]R. P. Feynman, *High Energy Collisions,* edited by C. N. Yang *et al.* (Gordon and Breach, New York, 1970).

[7]K. Wilson, Cornell Report No. CLNS-131, 1970 (unpublished).

[8]J. D. Bjorken, invited talk, American Physical Society Divisional Meeting, Rochester, New York, 1971 [SLAC Report No. SLAC-PUB-974 (unpublished)].

[9]A. Mueller, Phys. Rev. D 2, 2963 (1970).

[10]C. DeTar, C. E. Jones, F. E. Low, J. H. Weis, J. E. Young, and C.-I Tan, Phys. Rev. Letters 26, 675 (1971).

[11]E. L. Berger and A. Krzywicki, Phys. Letters 36B, 380 (1971).

[12]W. Pauli and M. Fierz, Nuovo Cimento 15, 1 (1938); D. Ito and H. Tanaka, Suppl. Nuovo Cimento 7, 91 (1958).

[13]O. Czyzewski and A. Krzywicki, Nuovo Cimento 30, 603 (1963).

[14]A. Krzywicki, Nuovo Cimento 32, 1067 (1964).

[15]A. Białas and Th. W. Ruijgrok, Nuovo Cimento 39, 1061 (1965).

[16]J. Bartke, Lectures at the International School of Elementary Particle Physics, Herceg-Novi, Strasbourg-Belgrad, 1970 (unpublished).

[17]R. H. Milburne, Rev. Mod. Phys. 27, 1 (1955).

[18]C. E. DeTar, Phys. Rev. D 3, 128 (1971).

[19]A. Pignotti, in *Proceedings of the Colloquium on Multiparticle Dynamics, University of Helsinki, 1971,* edited by E. Byckling *et al.* (Univ. of Helsinki Press, Helsinki, 1971).

[20]R. C. Arnold and P. E. Heckman, Phys. Rev. 164, 1822 (1967).

[21]R. C. Hwa, Phys. Rev. Letters 26, 1143 (1971).

[22]M. Jacob and R. Slansky, Phys. Letters 37B, 408 (1971); and Phys. Rev. D 5, 1847 (1972).

[23]A. Krzywicki, in *Proceedings of the Colloquium on High Multiplicity Hadronic Interaction, Paris, 1970,* edited by A. Krzywicki *et al.* (Ecole Polytechnique, Paris, 1970).

[24]F. Lurçat and P. Mazur, Nuovo Cimento 31, 149 (1964), hereafter called LM.

[25]A. Krzywicki, J. Math. Phys. 6, 485 (1965).

[26]F. Turkot, in *Proceedings of the Topical Conference on High Energy Collisions of Hadrons, CERN, 1968* (CERN, Geneva, 1968), Vol. 1.

[27]Y. A. Chao, Nucl. Phys. B40, 475 (1972).

[28]F. Cerulus, Nuovo Cimento 19, 528 (1961).

[29]J. Shapiro, Suppl. Nuovo Cimento 18, 40 (1960).

[30]W. Magnus, F. Oberhettinger, and R. P. Soni, *Formulas and Theorems for the Special Functions of Mathematical Physics* (Springer-Verlag, New York, 1966).

[31]See, for example, A. I. Khinchin, *Mathematical Foundations of Statistical Mechanics* (Dover, New York, 1949).

[32]P. P. Srivastava and G. Sudarshan, Phys. Rev. 110, 765 (1958).

[33]D. Horn and R. Silver, Phys. Rev. D 2, 2082 (1970).

[34]H. A. Kastrup, Nucl. Phys. B1, 309 (1967).

[35]See, for example, T. L. Saaty and J. Bram, *Nonlinear Mathematics* (McGraw-Hill, New York, 1964).

[36]L. Caneschi and A. Schwimmer, Phys. Rev. D 3, 1588 (1971).

[37]A. Białas and K. Zalewski, Nucl. Phys. B42, 325 (1972).

[38]See, for example, L. Van Hove, in *Proceedings of the Colloquium on Multiparticle Dynamics,* Ref. 19.

[39]D. Smith, thesis, LBL Report No. UCRL-20632, 1971 (unpublished).

[40]H. Bøggild *et al.*, Nucl. Phys. B27, 285 (1971).

[41]Saclay-Serpukhov Collaboration, Mirabelle Experiment at 69 GeV/c, 1972 (unpublished).

[42]L. W. Jones *et al.*, Nucl. Phys. B43, 477 (1972).

[43]The ISR points are estimated from $pp \to \gamma X$ data (Ref. 48); G. Charlton and G. Thomas, Phys. Letters (to be published).

[44]M. LeBellac, Lett. Nuovo Cimento 2, 437 (1971); J. Ellis, J. Finkelstein, and R. D. Peccei, SLAC Report No. SLAC-PUB-1020 (unpublished).

[45]A. K. Wroblewski, Rapporteur's talk in *Proceedings of the Fifteenth International Conference on High Energy Physics, Kiev, U.S.S.R., 1970* (Atomizdat, Moscow,

1971).
[46]M. Kugler and R. G. Roberts, Weizmann Institute Report No. WIS 71/51 Ph, 1972 (unpublished).
[47]The opposite point of view is assumed for example by M.-S. Chen and F. E. Paige, Phys. Letters 38B, 249 (1972).
[48]G. Neuhofer *et al.*, Phys. Letters 37B, 438 (1971).
[49]L. G. Ratner *et al.*, Phys. Rev. Letters 27, 68 (1971); A. Bertin *et al.*, Phys. Letters 38B, 260 (1972).

PHYSICAL REVIEW D VOLUME 6, NUMBER 7 1 OCTOBER 1972

Study of the Electromagnetic Structure of Δ(1236) via Photo- and Electrodisintegration of the Deuteron*

N. R. Nath and H. J. Weber
Department of Physics, University of Virginia, Charlottesville, Virginia 22901
(Received 31 May 1972)

The deuteron photo- and electrodisintegration processes $\gamma d \to \Delta\Delta$ and $ed \to e\Delta\Delta$ are shown to be probes of the electromagnetic properties of Δ(1236), on the basis of a Δ-exchange-reaction mechanism. The presence of the ΔΔ configuration in the deuteron, with an estimated probability of 1%, yields a photon cross section of the order of 1 μb at 1–2 GeV photon energy.

I. INTRODUCTION

Until recently, theoretical treatments of the deuteron ignored the excited states of the nucleon. Indeed, in the low-energy regime, the deuteron is adequately described by means of a nonrelativistic wave function with pointlike nucleons of essentially static properties as its constituents. In reactions involving high momentum transfer, the mutual excitation of nucleons is no longer expected to be negligible. If the low-lying excited states of the nucleon are treated as elementary particles on an equal basis with the nucleon ground state, then such isobars would, in a nonrelativistic description, give rise to isobar configurations in the deuteron wave function.

Kisslinger and Kerman[1] were the first to introduce a D-state ($N(938), N'(1688)$) configuration in the ground-state wave function of the deuteron via an isobar exchange mechanism for proton-deuteron elastic scattering which was designed to support the backward peak at a proton energy of ~1 GeV. They picked $F_{15}(1688)$ as a suitable exchange mechanism, rather than any other low-lying $T=\frac{1}{2}$ isobar on an analogy with the Regge-pole model of πp scattering. Subsequently, isobar configurations have been used[2] for the magnetic moments of the deuteron and ^{3}He in order to account for the small discrepancies between the experimental values and those provided by conventional nuclear theory. In the context of weak interactions,[3] isobar wave functions give rise to similar corrections. Relying on isospin invariance, forward proton production in $\pi^- d$ collisions has been proposed in Ref. 4 as a direct test of the ΔΔ configuration in the deuteron assuming a Δ-exchange mechanism at high incident energy.

Here our objective is different: Assuming the ΔΔ configuration to be present in the deuteron with a probability of 1%, we propose the virtual decay process $d \to \Delta\Delta$ as a means to study electromagnetic properties of Δ(1236). For example, by high-energy electron scattering from deuterium one may observe $e\Delta$ scattering through $e + (d \to \Delta\Delta) \to e + \Delta + \Delta$(spectator). This method is similar to that used to determine the form factors of the neutron. It seems promising in view of the lack of any experimental information on electromagnetic vertices ($N^*N^*\gamma$) of excited hadron states. A particularly interesting parameter is the static magnetic moment of Δ(1236) which is predicted by the quark model[5] to be $e_\Delta \mu_p$. Radiative $\pi^+ p$ scattering has been suggested earlier[6] as a means to determine the magnetic moment of $\Delta^{++}(1236)$, but no results have been reported to date.

If we consider Δ^{++} production, nucleon exchange is forbidden by charge conservation. For outgoing $\Delta^+\Delta^0$, isospin conservation at the deuteron vertex leads to the same result. Hence, we restrict our attention to the reactions

$$\gamma + d \to \Delta^{++} + \Delta^-, \tag{1}$$

$$e + d \to e + \Delta^{++} + \Delta^-, \tag{2}$$

as shown in Fig. 1. In order to extract the electromagnetic moments of $\Delta^{++}(1236)$ our analysis pertains mainly to the neighborhood of the maximum accessible mass $(t_{max})^{1/2} = m_d - m_\Delta \sim 0.64$ GeV of the